https://doi.org/10.1007/s41230-017-7078-y

Coating process of multi-material composite sand mold 3D printing

Zhong-de Shan[1], *Zhi Guo[1, 2], Dong Du[2] and Feng Liu[1]
1. China Academy of Machinery Science & Technology, Beijing 100044, China
2. Department of Mechanical Engineering, Tsinghua University, Beijing 100084, China

Abstract: Sand mold 3D printing technology is an advanced manufacturing technology which has great flexible manufacturing ability. A multi-material composite sand mold can control the temperature field of metallic parts during the pouring process, while the current sand mold 3D printing technology can only fabricate a single material sand mold. The casting temperature field can not be adjusted by using single sand mold material with isotropous heat exchange ability during the pouring process. In this work, a kind of novel coating device was designed. Multi-material composite sand molds could be manufactured using the coating device according to the casting process demands of the final parts. The influences of curing agent content, coating velocity and scraper shape on compactness and surface roughness of the sand layer (silica sand and zircon sand) were studied. The shapes and sizes of transition intervals of two kinds of sand granules were also tested. The results show that, with the increase of the added volume of curing agent, the compactness of sand layer reduces and the surface roughness value rises. With the increase of the velocity of the coating device, the compactness of sand layer reduces and the surface roughness value rises similarly. In addition, the scraper with a dip angle of 72 degrees could increase the compactness value of the sand layer. The criteria of quality parmeters of the coating procedure are obtained. That is, the surface roughness (δ) of sand layer should be equal to or lesser than half of main size of the sand particles (D_m). The parameter H of the coating device which is the distance between the base of hopper and the surface of sand layer impacts the size of transition zone. The width of the transition zone is in direct proportion to the parameter H, qualitatively. Through the optimization of the coating device, high quality of multi-material sand layers can be obtained. This will provide a solution in manufacturing the multi-material composite sand mold.

Key words: multi-material composite sand mold; 3D printing; coating process; self-adaption coating device

CLC numbers: TG231.6 **Document code:** A **Article ID:** 1672-6421(2017)06-498-08

With the development of additive manufacturing, more and more attention is paid to the flexible manufacturing ability of 3D printing technology. The 3D printing technology is based on the principle of layered manufacturing. Firstly, the CAD file of the final part is converted to the STereo Lithography (STL) file, and then the STL file is converted to the Common Layer Interface (CLI) file which contains the geometric information of each layer. Finally, the part is built layer by layer until it is completed. Sand mold 3D printing technology is one kind of indirect metallic additive manufacturing technology. The CAD model of the casting mold needs to be firstly reversed out by the CAD model of the metal part [1, 2]. Currently, sand mold 3D printing technology is mainly divided into two types: one is based on the principle of selective laser sintering, the other is based on the principle of micro-droplet [3]. The former normally uses a laser to melt the film coating on the surface of sand particles, however the latter normally uses a droplet nozzle to spray the adhesives to the surface of sand particles which are premixed with a curing agent, and the particles are bonded together when the adhesives react with the curing agent [4, 5]. The adhesives used in sand mold 3D printing mainly include furan resin, phenolic resin and inorganic adhesives based on silicate and phosphate [6–8].

The two types of sand mold 3D printing technologies mentioned above are both based on the powder bed to fabricate the casting mold. The forming process includes many fabricating procedures, such as storage, supply, coating, and recovery of sand particles. The quality of the coating procedure has a great influence on the performance of the sand mold. The compactness and surface roughness of the sand layer are two key parameters to measure the quality of the coating procedure [9, 10]. The strength of the sand mold is affected by the added volume of adhesives and the compactness

*** Zhi Guo**
Male, 1988, doctoral candidate. His research mainly focuses on digital rapid prototyping equipment.
E-mail: guo-z14@mails.tsinghua.edu.cn
Received: 2017-06-05; Accepted: 2017-08-10

of the sand layer. Previous studies [11] have shown that the greater the compactness value, the greater the strength value of the sand mold. Therefore, the stable operation of the coating device has a great influence on the continuity and reliability of the sand mold manufacturing process. Currently, there exist three types of coating device: roller style, scraper style and travelling hopper style [12]. The coating process and apparatus used in polymeric and metallic additive manufacturing have been studied by many scholars [13-15], however little work has been done concerning sand mold 3D printing. The concept of a multi-material composite sand mold was proposed in the research of patternless casting based on the principle of sand mold milling. That is, many divided sand molds with different kinds of foundry sand have been assembled together to form an integrated sand mold according to the differences of temperature and stress fields during the processes of the filling and solidification process of molten metal [16]. Multi-material composite sand mold can control the temperature field of the metallic parts during the pouring process according to the plan of casting. Currently, sand mold 3D printing technologies only fabricate a single material sand mold. The casting temperature field could not be adjusted by using single sand mold material with isotropous heat exchange ability during the pouring process. The flexible manufacturing ability of sand mold 3D printing technology has been therefore limited.

In order to solve the current problems in sand mold 3D printing technology, a novel coating device was designed in this work. Two or three kinds of sand particles could be coated in one layer. This provides an approach to achieve fabricating a multi-material composite sand mold. The influences of curing agent content, coating velocity, and scraper shape on compactness and surface roughness were quantitatively studied through coating procedure testing. A coating procedure of multi-material sand layer was also researched.

1 Test materials and research method

1.1 Test materials and methods

The silica sand and zircon sand used in the test were both foundry sands available on the market. The sifting method was used to measure the granule sizes of silica sand and zircon sand. The size of the sand granules used in sand mold 3D printing is usually approx. 100 mesh screening. The particle size distributions of silica sand and zircon sand are shown in Fig.1. An optical microscope (OLYMPUS BX51M) was used to observe the granule shape of the sample, as shown in Fig. 2. From Figs. 1 and 2, it can be seen that the particle sizes of zircon sand are smaller than that of the silica sand, and both of them have a similar granule shape.

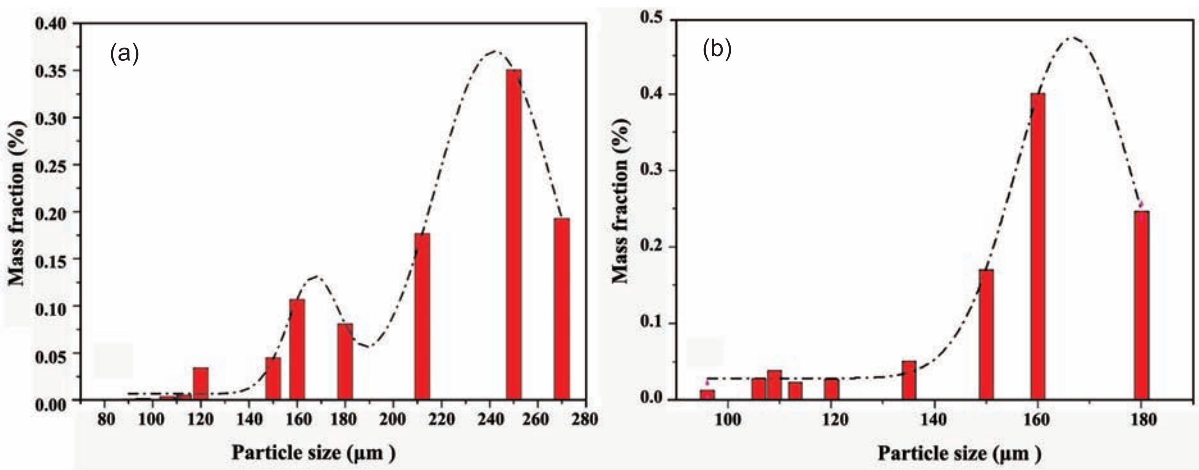

Fig. 1: Particle size distributions of silica sand (a) and zircon sand (b)

During the process of sand mold printing, the sand particles needed to be premixed with a curing agent. The curing agent used in this test was the mixture of p-toluenesulfonic acid and sulfuric acid. It is well known that as the added volume of curing agent increases, the flowability of sand particles and the quality of the coating procedure reduces significantly [20-22]. Test samples with different ratios of curing agent were prepared according to Table 1, where S is a ratio of curing agent weight to sand particle weight, that is the added volume of curing agent.

1.2 Design of self-adaption coating device

The self-adaption coating device employed a kind of combinational design of scraper style and travelling hopper style. In order to achieve multi-material sand layer coating, the coating device has many channels with an independent open-close function, as shown in Fig. 3. The removable plate, driven by the air cylinder, was used to open or close the channel. The self-adaption coating device could use different kinds of sand particles on the same layer under the control of the computer. During the coating procedure of the multi-material sand layer, two of the same self-adaption coating devices were used. One was filled with silica sand particles, the other was filled with zircon sand particles. The multi-material sand layer was obtained by opening or closing the same channel in the two coating devices in complementarity at the same time and the same place.

During the coating procedure, the connection interval

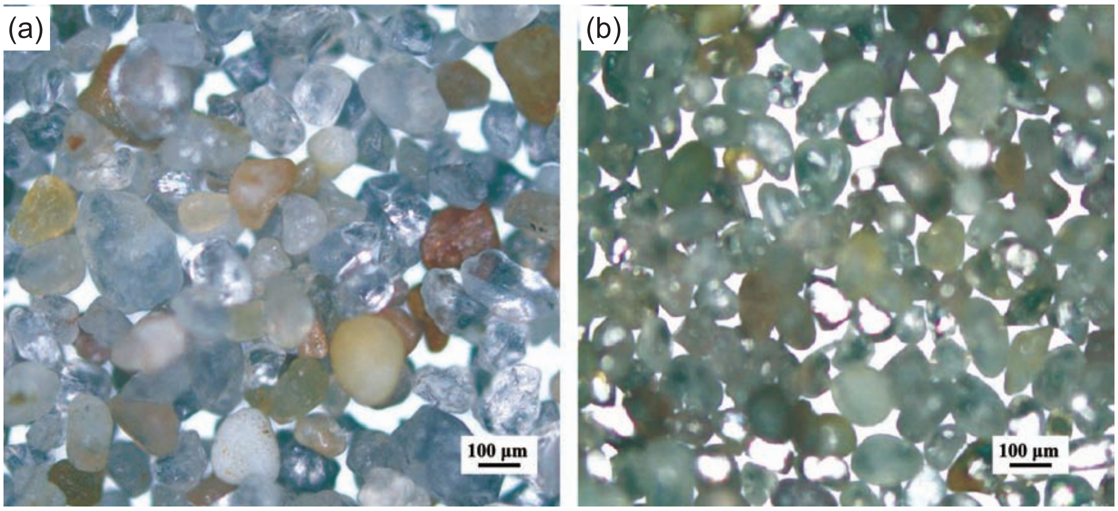

Fig. 2: Microscope figures of granule shape: (a) silica sand, (b) zircon sand

Table 1: Test sample and added volume of curing agent

Test sample	The added volume of curing agent, *S* (%)				
Silica sand	0	0.3	0.5	0.7	0.9
Zircon sand	0	0.1	0.2	0.3	0.4

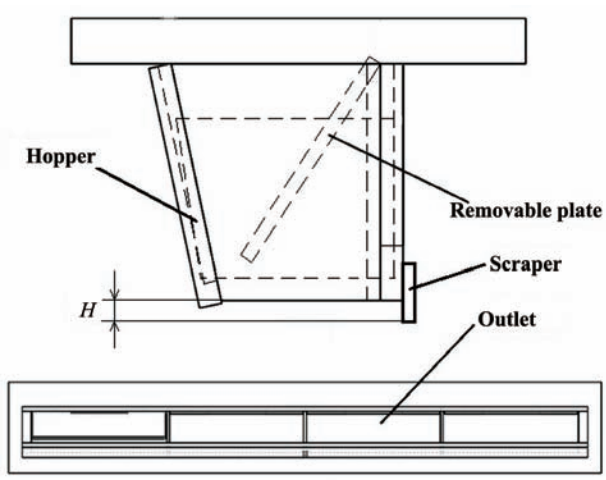

Fig. 3: Self-adaption coating device

between silica sand and zircon sand had two connection styles: one is the connection interval for one sand band which refers to the opening style of coating device, the other is the connection interval between the two sand bands which refers to the channel size of coating device and flowability of sand particles.

1.3 Quality measurement of coating procedure

The digital sand mold 3D printing machine developed by China Academy of Machinery Science & Technology was used to study the coating procedure. The quality of the coating procedure mainly depends on compactness D and surface roughness δ of sand layer. D is the ratio of packing density to real density of sand particles, as shown in the following equation:

$$D = \frac{\rho_0}{\rho} \tag{1}$$

where, ρ_0 (kg·m^{-3}), ρ (kg·m^{-3}) denote the packing density and real density of sand particles, respectively.

The light-section method was used to study the surface roughness δ of coated sand layer. The schematic of the test is shown in Fig. 4 [17-19], where $\theta \approx 90°$. The universal program software LABVIEW was used to manipulate test figures to extract the geometric edge feature points of sand layer. The profile arithmetic average error Ra was used to characterize the surface roughness of sand layer. In the test, the surface roughness δ of the sand layer is the average of three Ra values which are measured from different locations in the same sand layer.

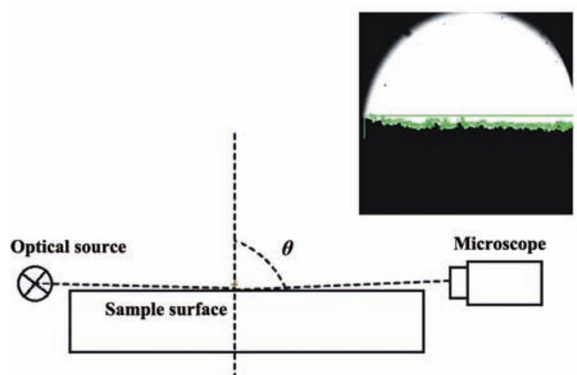

Fig. 4: Schematic of light-section method to measure surface roughness of sand layer

2 Coating procedure and quality of sand layer

2.1 Sand layer compactness

2.1.1 Influence of added volume of curing agent on sand layer compactness

The flowability of sand particles is influenced by the added volume of curing agent. Many studies [20–22] showed that with the increase of the moisture content of particles, the cohesions among particles increase, causing the flowability reduction of sand particles. Poor flowability of sand particles leads to low compactness of the sand layer during the coating process. Results on the influences of the content of curing agent on the compactness of silica and zircon sand layer are shown in Fig. 5. Figure 5(a) shows the influence of curing agent content on compactness of the silica sand layer, and Figure 5(b) shows the influence of curing agent content on compactness of the zircon sand layer. It can be found from Fig. 5(a) with Fig. 5(b), that, with the increase of content of curing agent, the compactness of the sand layer reduces seriously. This change rule has good consistency under different coating velocities. The compactness of the zircon sand layer is better than that of the silica sand layer. This results from two kinds of different particle sizes as well as their distributions. The average particles size of zircon sand is smaller than the silica sand, while the compactness of particles is inversely proportional to the particles size in the condition of the same filling volume.

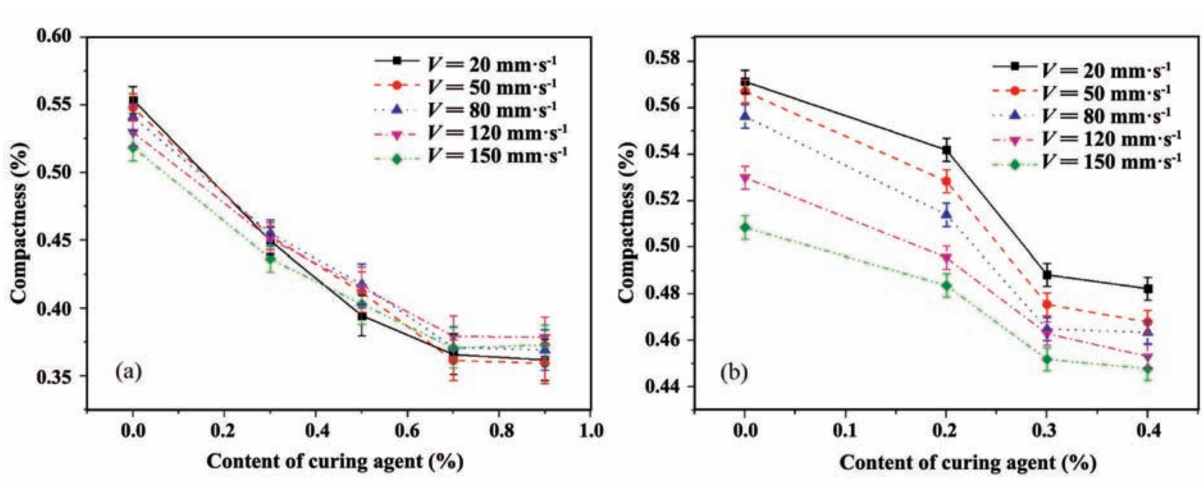

Fig. 5: Influences of added volume of curing agent on compactness of silica sand layer (a) and zircon sand layer (b)

2.1.2 Influence of coating velocity on sand layer compactness

Coating velocity is the key parameter for manufacturing efficiency. Figures 6 (a) and (b) show the test results of influence of coating velocity on compactness of silica sand and zircon sand layers, respectively. The results show that the compactness of zircon sand layer is much more sensitive to the coating velocity than that of silica sand layer. With the increase of coating velocity, the compactness of sand layer gradually reduces. For the test sample with high content of curing agent, such as $S_{silica} \geqslant 0.5\%$ and $S_{zircon} \geqslant 0.3\%$, the influence of coating velocity on the sand layer compactness is slighter than the test sample with low content of curing agent, such as $S_{silica} < 0.5\%$ and $S_{zircon} < 0.3\%$. This indirectly shows that the added volume of curing agent in sand particles has greater influence on the compactness of sand layer than the coating velocity. During the coating procedure, sand particles are in a state of bonding or friction. The curing agent increases the cohesion among particles. Meanwhile, the surface state of the particles changes from dry to wet, which makes the friction forces smaller

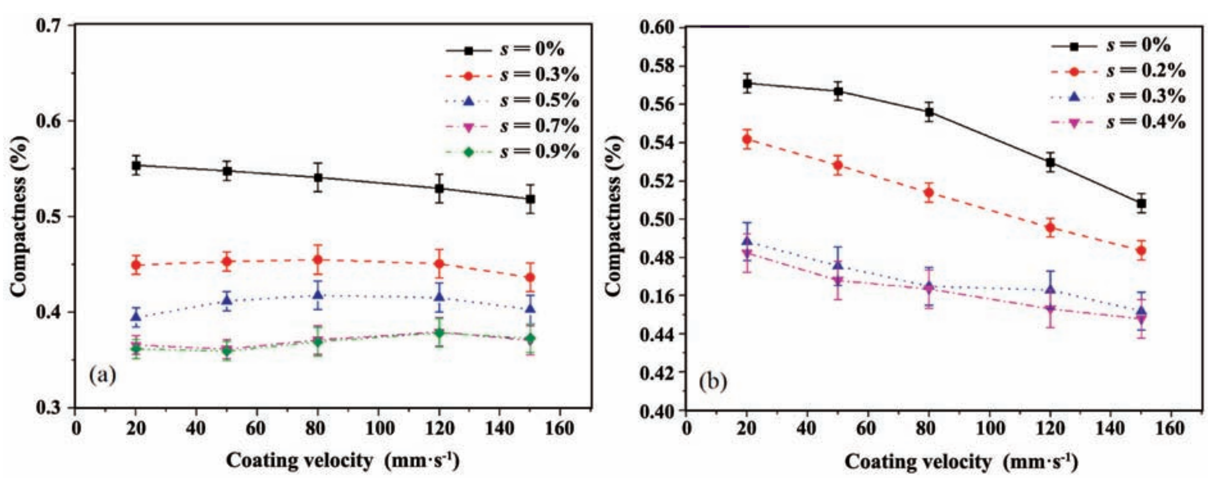

Fig. 6: Influences of coating velocity on compactness of silica sand layer (a) and zircon sand layer (b)

between particles [23, 24]. Because of the great cohesion among particles, many small particles aggregate to form a large particle, which causes the lower compactness of the sand layer.

Silica sand have larger particle sizes and higher contents of curing agent, corresponding to higher cohesions and lesser frictions among particles. So, the compactness of the sand layer is insensitive to the change of coating velocity [14, 23, 24]. On the contrary, the zircon sand have smaller particle sizes and lower contents of curing agent, corresponding to lesser cohesions and higher frictions among particles. The compactness of the sand layer is sensitive to the change of coating velocity.

2.1.3 Influence of scraper shape on compactness of sand layer

During the coating procedure, the scraper of the coating device will contact with sand particles, and exert different forces on the sand particles with different contact angles. Therefore, the influences of the scraper with 0° and 72° dip angles on the compactness of the sand layer were studied. Coating velocity was set as 50 mm·s^{-1}. The results are shown in Fig. 7. It can be seen that the scraper with 72° dip angle is beneficial for improving the compactness of the sand layer, and the greater the content of curing agent in the sand particles, the more obvious the effect of the scraper with dip angle is to improve the compactness of sand layer. Actually, the coating procedure is a shear motion of sand particles under the function of scraper. The scraper with a 72° dip angle will exert vertical pressure on the sand layer during the coating procedure.

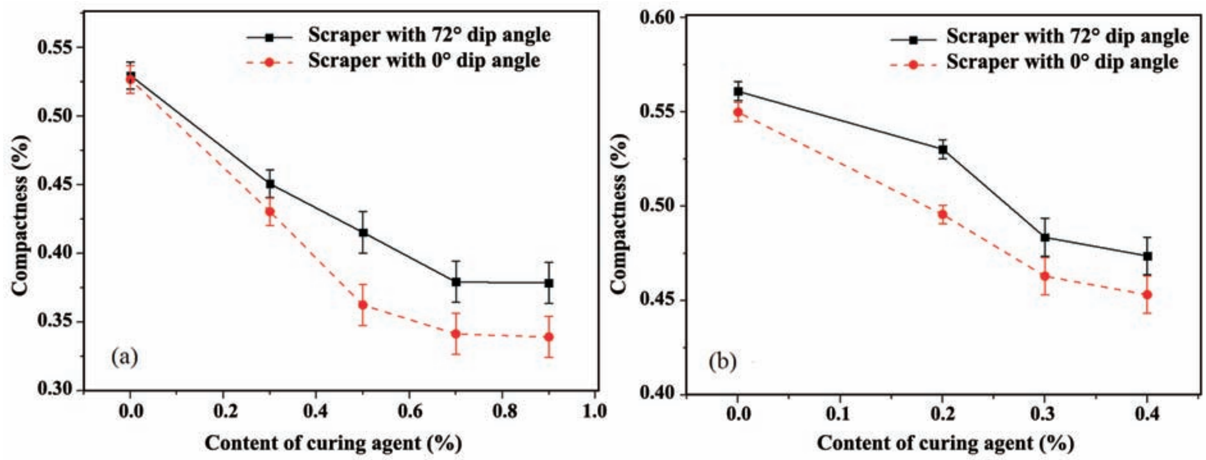

Fig. 7: Influence of scraper shape on compactness of silica sand layer (a) and zircon sand layer (b)

2.2 Surface roughness of sand layer

2.2.1 Influence of added volume of curing agent on surface roughness of sand layer

The surface roughness of the sand layer is a key parameter to characterize the smoothness of the sand layer [15]. Figure 8 shows the influences of added volume of curing agent on the surface roughness of the sand layer with a coating velocity of 50 mm·s^{-1}. The surface roughness changed with added volume of curing agent. The surface roughness value of the silica sand layer is greater than that of the zircon sand layer, and the surface roughness of the sand layer is in proportion to the added volume of curing agent. The main reason is that the particle size of silica sand is larger than that of the zircon sand particles. The main size of silica sand particles, $D_{m,silica}$, concentrated on ~240 μm, while the main size of zircon sand particles, $D_{m,zircon}$, concentrated on ~170 μm (see Fig. 1). Through curve fitting, the relationship between the surface roughness δ and the content of curing agent S was obtained (Table 2). Figure 9 shows the test results of the influences of curing agent content on the surface roughness, with a coating velocity of 50 mm·s^{-1}. It shows that

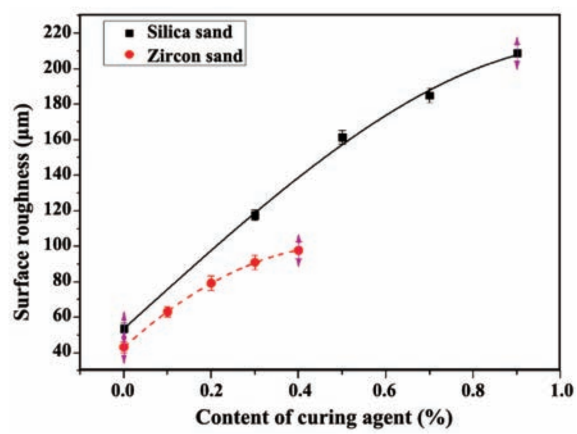

Fig. 8: Influence of added volume of curing agent on surface roughness of sand layer

when the added volumes of curing agent in silica sand and zircon sand, i. e. S_{silica} and S_{zircon}, were both equal to 0%, the surface roughness δ of two kinds of sand layers was 53.9 μm and 43.3 μm, respectively, which are close to 60 μm and 42.5 μm which are the $D_m/4$ of silica sand particles and zircon sand particles, respectively. This implies that the smoothness of the sand layer is good. But when $S_{silica} \geqslant 0.5\%$ and $S_{zircon} \geqslant 0.3\%$, the surface roughness δ for silica sand particles and zircon sand particles is greater than 120 μm and 85 μm, respectively, which are the $D_m/2$ of silica sand particles and zircon sand particles. A wave phenomenon occurs in the surface of sand layer, and affects the smoothness of the sand layer. In Fig. 6, when $S_{silica}\geqslant0.5\%$ and $S_{zircon}\geqslant0.3\%$, the compactness of silica sand layer is $D_s\leqslant0.4$, and the compactness of zircon sand layer is $D_z\leqslant0.5$.

Table 2: Relationship between surface roughness δ and content of curing agent, S

Test sample	Function ($\delta = a + b \times S + c \times S^2 + d \times S^3$)			
	a	b	c	d
Silica sand	53.75	222.36	3.12	-66.74
Zircon sand	43.19	224.04	-217.46	-

2.2.2 Influence of coating velocity on surface roughness of sand layer

When the added volume of curing agent is equal to 0%, the influence of coating velocity on the surface roughness of sand layer is shown in Fig. 10. Results show that the coating velocity has greater influence on the surface roughness of silica sand layer than on that of the zircon sand layer. Through curve fitting, the relationship between surface roughness δ and coating velocity V is obtained, as shown in Table 3. Figure 11 shows the test results of the influences of coating velocity on the surface roughness of the sand layer, when the added volume of curing agent is equal to 0%. With the increase of coating velocity ranging from 20 to 150 $mm{\cdot}s^{-1}$, the surface roughness changes

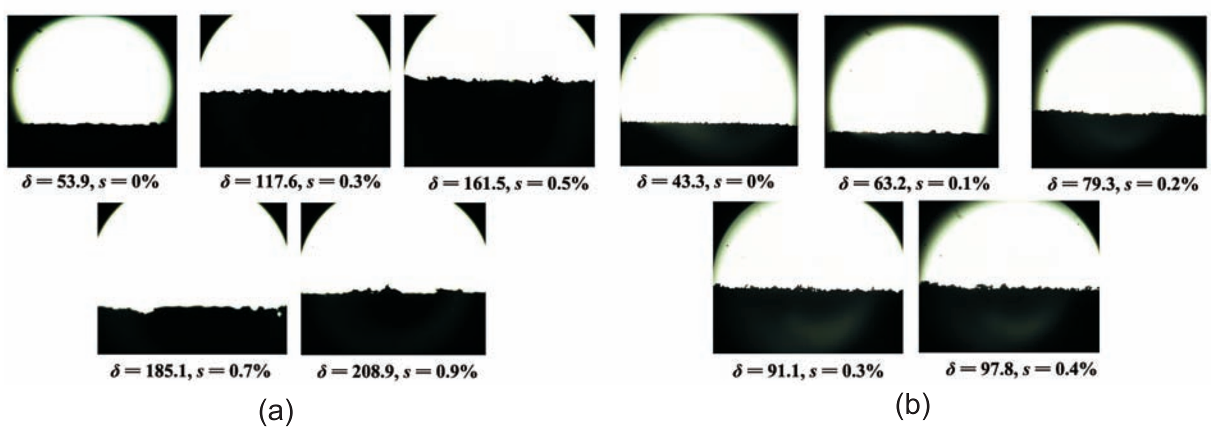

Fig. 9: Surface roughness of sand layers with different curing agent contents measured by light-section method: (a) silica sand layer, (b) zircon sand layer

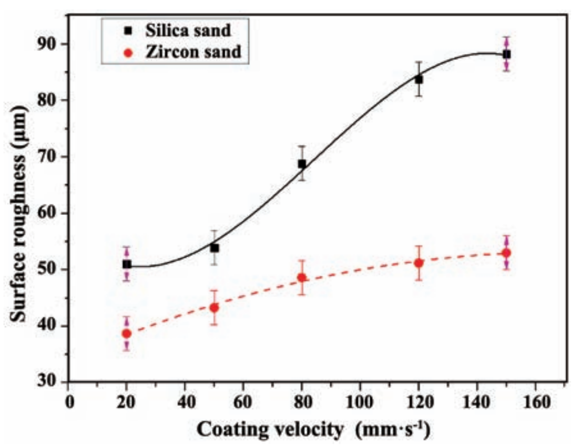

Fig. 10: Influence of coating velocity on surface roughness of sand layer

Table 3: Relationship between surface roughness δ and coating velocity V

Test sample	Function ($\delta = a + b \times V + c \times V^2 + d \times V^3$)			
	a	b	c	d
Silica sand	56.16	-0.48	0.011	-4.53E-05
Zircon sand	34.35	0.22	-6.62E-04	-

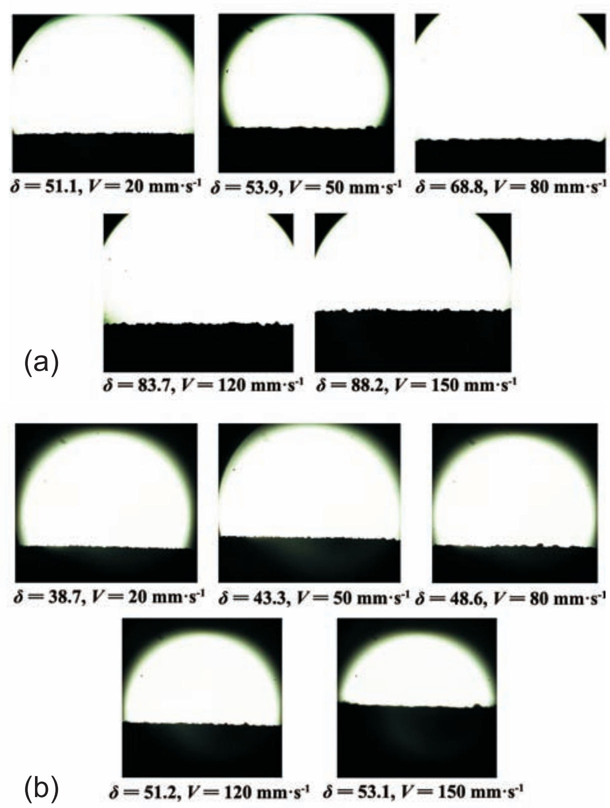

Fig. 11: Surface roughness of sand layers with different coating velocities measured by light-section method: (a) silica sand layer, (b) zircon sand layer

from $D_m/4$ to $D_m/2$. When the surface roughness δ is less than $D_m/2$, the better smoothness of the sand layer can be obtained.

2.3 Coating procedure research for multi-material sand layer

The adaptive coating procedure of multi-material sand particles is the key to accomplish the manufacture of a composite sand mold. The coating procedure of simultaneous coating silica sand and zircon sand particles was studied using the above mentioned self-adapting coating device. In this research, it was key to control the size of the transition zone between the two kinds of sand. The self-adapting coating device consists of four independent sand outlets with a size of 150 mm. The silica sand test sample with 0.3% curing agent was added to a single sand hole to form a sand band. The width of the sand band was 177 mm, while the band width of the zircon sand test sample with 0.2% curing agent was 180 mm.

The coating of multi-material composite sand layer is divided into two parts: the connection of different materials in different sand bands and the connection of different materials in the same sand band. The adaptive coating procedure for the multi-material sand layer is made up of two self-adapting coating devices with the same structure and different sand particles. The outlets of two coating devices are complementary to open or close at the same time to complete the coating of the multi-material composite sand layer. Figure 12 shows the test results. Figure 12 (a) is the ideal composite sand layer, and Figure 12 (b) is the real composite sand layer.

In Fig. 12, A represents the silica sand particles, B represents the zircon sand particles. Experimental measurements show that the bandwidths of silica sand particles and zircon sand particles are both between 130–140 mm. The transition zone between silica sand particles and zircon sand particles appears at the junction of silica sand particles and zircon sand particles. The size of the transition zone is affected by the flowability of sand particles and the distance H between the bottom of the coating hopper and the surface of the sand layer (Fig. 3). When the removable plate is opened, sand particles are scattered down from the outlet of the coating device. The edge shape and size of sand band are determined by the flowability and amount of sand particles. The width of the transition zone is in direct proportion to the flowability of sand particles and the parameter H.

The transition zone is connected by different sands in the same band, and needs two self-adapting coating devices to open and close the same outlet at the same place to complete the coating of multi-material composite sand layers. The test result is shown in Fig. 13. It shows that after the coating of silica sand particles, a semicircle edge shape will be formed. In this condition, if the zircon sand particles continue coating in the place where the silica sand particles are stopped from coating, a semicircle transition zone will be created. The test shows that the size of the transition zone is affected by the amount of sand deposited after the outlet of the coating device is closed. The more the waste sand particles, the greater the transition zone size. The amount of waste sand particles is affected by the opening and closing style of the coating device. In this work, the opening and closing style of the coating device employs a type of gate valve. An interval of deposited sand particles is formed after closing the removable plate. These deposited sand particles forms the semicircular transition zone during the coating process. A smaller transition zone can be realized by optimizing the opening and closing style of the coating device, thereby improving the accuracy of the connection of different sands in the same band.

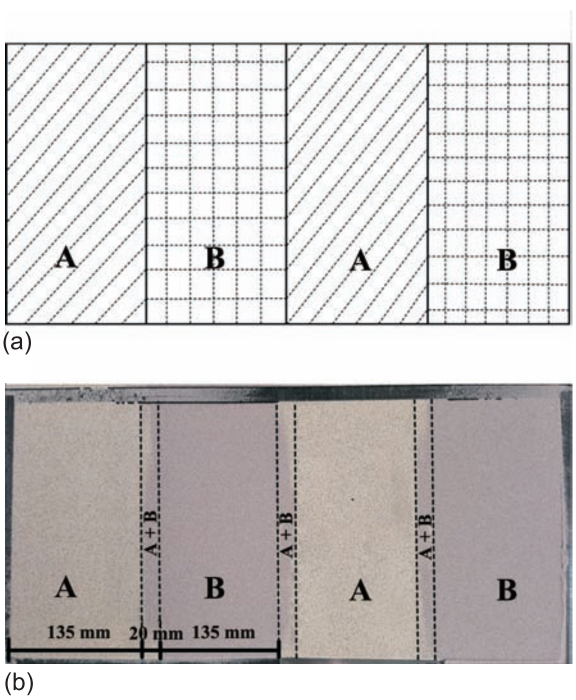

Fig.12: Connection interval of multi-material sand layer between different sand bands: (a) ideal composite sand layer, (b) real composite sand layer

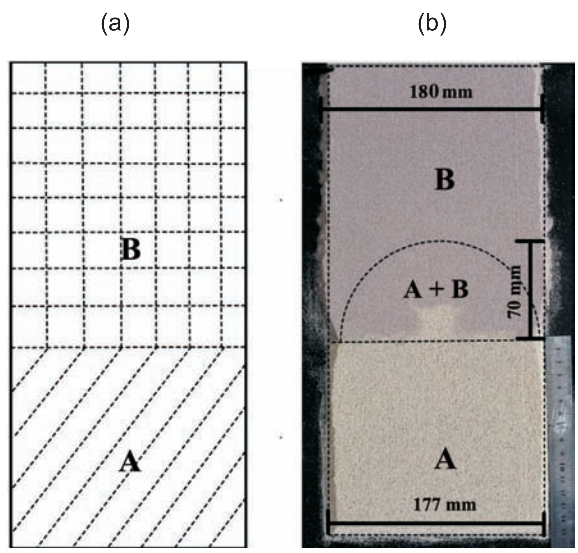

Fig. 13: Connection interval of multi-material sand layer in one sand band:(a) ideal composite sand layer, (b) real composite sand layer

3 Conclusions

The quality of the coated sand layer has a great influence on the strength of the sand mold made by 3D printing technology. Through the coating procedure test, the influence of the content of curing agent, coating velocity and scraper shape on compactness and surface roughness of the sand layer have been deeply studied. Based on the research of the single sand particle coating procedure, the multi-material sand particle self-adaptive coating procedure has also been researched. Results show as follows:

(1) The curing agent content and coating velocity are in inverse proportion to the compactness of sand layer. In addition, the dip angle scraper can increase the compactness of sand layer to some extent.

(2) The criteria of surface roughness of the sand layer are obtained in the test, which is $\delta \leqslant D_m/2$. Correspondingly, the curing agent content should satisfy the condition: $S_{silica} \leqslant 0.5\%$ and $S_{zircon} \leqslant 0.3\%$, and for the silica sand layer, $\delta=53.75+222.36S+3.12S^2-66.74S^3$ and $\delta=56.16-0.48V+0.011V^2-4.53\times10^{-5}V^3$; for the zircon sand layer, $\delta=43.19+224.04S-217.26S^2$ and $\delta=34.35+0.22V-6.22\times10^{-4}V^2$. According to the criteria of surface roughness of sand layer, the criteria of compactness of sand layer for silica and zircon sand are $D_s>0.4$ and $D_z>0.5$, respectively.

(3) There are two kinds of sand particles mixed in the transition zone, the semicircle edge shape will be formed after the coating of silica sand particles, and the sizes of transition zone are determined by the design parameter H and the opening style of the coating device. The size of the transition zone can be reduced by optimizing the opening and closing style of the coating device, and high quality multi-material sand layers could be obtained.

References

[1] Elena B, Andrea G. 3D printing technique applied to rapid casting. Rapid Prototyping Journal, 2007, 13(3): 148–155.
[2] Ian C, David B, Ian G. Additive manufacturing: rapid prototyping comes of age. Rapid Prototyping Journal, 2012, 18(4): 255–258.
[3] Dimitrov D, Schreve K, Beer D N. Advances in three dimensional printing – state of the art and future perspectives. Rapid Prototyping Journal, 2006, 12(3): 136–147.
[4] Daniel G, Bastian H, Fohannes F G, et al. Continuous 3D-printing for additive manufacturing. Rapid Prototyping Journal, 2014, 20 (4): 320–327.
[5] Zhu Peilan, Xu Zhifeng, Yu Huan, et al. Progress of Rapid Technology without Mold in Precision Sand Casting. Special Casting & Nonferrous Alloys, 2013, 33(2): 136–140. (In Chinese)
[6] Zhao Hongfeng, Shan Zhongde, Liu Feng, et al. The patternless sand mold printing with ester cured alkaline phenol resin. Foundry, 2016, 65(4): 309–312. (In Chinese)
[7] Xing Jinlong, He Long, Han Wen, et al. Research on Synthesis and Performance of A High-Strength and High-Temperature Resistant Phenolic Resin Used in Three Dimensional Printing of Sand Mold. Foundry, 2016, 65(10): 966–969. (In Chinese)
[8] Xing Jinlong, He Long, Han Wen, et al. Research on Synthesis and Performance of Inorganic Binder Used in Three Dimensional Printing of Sand Mold. Foundry, 2016, 65(9): 851–854. (In Chinese)
[9] Shi Y, Li Z, Sun H, et al. Effect of the properties of the polymer materials on the quality of selective laser sintering parts. Proceedings of the Institution of Mechanical Engineers Part L Journal of Materials Design and Applications, 2004, 218(3): 247–252.
[10] Kruth J P, Leny G, Schnidel R, et al. Consolidation of polymer powders by selective sintering. In: Proc. PMI2008, Ghent, Belgium, September 2008.
[11] Vanhooreweder B, Deconinck F, et al. Microstructural Characterisation of SLS-PA12 Specimens Under Dynamic Tension/Compression Excitation. Polymer Testing, 2010, 29 (3): 319–326.
[12] Yan Naisheng, Lin Feng, Qi Haibo, et al. Study on Controllable Vibration Powder Spreading System in Electron Beam Selective Melting. China Mechanical Engineering, 2010, 21(19): 2379–2382. (In Chinese)
[13] Mindt H W, Megahed M, Lavery N P, et al. Powder Bed Layer Characteristics: The Overseen First-Order Process Input. Metallurgical and Materials Transactions A, 2016, 47(8): 3811–3822.
[14] Shinichi Y, Toshihiko U, Yutaka K. Numerical Simulation for the Friction Mechanism of A Powder Bed Using Two-Dimensional Distinct Element Method. Advanced Powder Technology, 2006, 17(3): 345–359.
[15] Eric J R, Parteli T P. Particle-based Simulation of Powder Application in Additive Manufacturing. Powder Technology, 2016, 288: 96–102.
[16] Shan Zhongde. Patternless casting. Beijing: China Machine Press, 2017. (In Chinese)
[17] Ped S E, Druzhinin P V. Automation of Surface Roughness Measurements. Measurement Techniques, 2015, 58(7): 752–756.
[18] Jakub S, Chiaki T. Evaluation of Surface Smoothness Using A Light-Sectioning Shadow Scanner. Journal of Wood Science, 2005, 51(3): 270–273.
[19] Kelkar A S, Kumbhar N N, Mulay A V. Surface Roughness Measurement of Parts Manufactured by FDM Process Using Light Sectioning Vision System. Journal of the Institution of Engineers, 2016, 1–5.
[20] Chen P, Yuan Zh, Shen X, et al. Flow Properties of Three Fuel Powders. Particuology, 2012, 10(4): 438–443.
[21] Ganesan V, Muthukumarappan K, Rosentrater K A. Flow Properties of DDGS with Varying Soluble and Moisture Contents Using Jenike Shear Testing. Powder Technology, 2008, 187(2): 130–137.
[22] Erica E, Jasmine O, Todd P, et al. Flowability of Moist Pharmaceutical Powders. Powder Technology, 2009, 189(3): 409–415.
[23] Opalinski I, Chutkowski M, Stasiak M. Characterizing moist food-powder flowability using a Jenike shear-tester. Journal of food engineering, 2012, 108(1): 51–58.
[24] Pablo J, Balasingam M, Gustavo V, et al. Flow and shear descriptors of preconsolidated food powders. Journal of Food Engineering, 2006, 72 (2): 157–166.

This work was financially supported by the National Excellent Young Scientists Fund (NO.51525503)